THE JOURNAL OF BIOLOGICAL CHEMISTRY
Vol. 279, No. 51, Issue of December 17, pp. 52869–52880, 2004
Printed in U.S.A.

Cytochrome c_{550} in the Cyanobacterium *Thermosynechococcus elongatus*

STUDY OF REDOX MUTANTS*

Received for publication, July 20, 2004, and in revised form, August 23, 2004
Published, JBC Papers in Press, September 22, 2004, DOI 10.1074/jbc.M408206200

Diana Kirilovsky‡§, Mercedes Roncel¶, Alain Boussac‡, Adjélé Wilson‡, Jorge L. Zurita¶, Jean-Marc Ducruet‡, Hervé Bottin‡, Miwa Sugiura‡, José M. Ortega¶, and A. William Rutherford‡

From the ‡Service de Bioénergétique, Departement Biologie Joliot-Curie, URA Consejo Superior de Investigaciones Cientificas 2096, CEA Saclay, 91191 Gif sur Yvette, France and the ¶Instituto de Bioquímica Vegetal y Fotosíntesis, Universidad de Sevilla y CSIC, Américo Vespucio 49, 41092 Sevilla, Spain

Cytochrome c_{550} is one of the extrinsic Photosystem II subunits in cyanobacteria and red algae. To study the possible role of the heme of the cytochrome c_{550} we constructed two mutants of *Thermosynechococcus elongatus* in which the residue His-92, the sixth ligand of the heme, was replaced by a Met or a Cys in order to modify the redox properties of the heme. The H92M and H92C mutations changed the midpoint redox potential of the heme in the isolated cytochrome by +125 mV and −30 mV, respectively, compared with the wild type. The binding-induced increase of the redox potential observed in the wild type and the H92C mutant was absent in the H92M mutant. Both modified cytochromes were more easily detachable from the Photosystem II compared with the wild type. The Photosystem II activity in cells was not modified by the mutations suggesting that the redox potential of the cytochrome c_{550} is not important for Photosystem II activity under normal growth conditions. A mutant lacking the cytochrome c_{550} was also constructed. It showed a lowered affinity for Cl^- and Ca^{2+} as reported earlier for the cytochrome c_{550}-less *Synechocystis* 6803 mutant, but it showed a shorter lived $S_2Q_B^-$ state, rather than a stabilized S_2 state and rapid deactivation of the enzyme in the dark, which were characteristic of the *Synechocystis* mutant. It is suggested that the latter effects may be caused by loss (or weaker binding) of the other extrinsic proteins rather than a direct effect of the absence of the cytochrome c_{550}.

Cytochrome c_{550} (cyt c_{550}),[1] present in cyanobacteria and red algae, was first discovered by Holton and Myers (1) as a soluble monoheme *c*-type cytochrome. The cyt c_{550} has a molecular mass of about 15 kDa, His/His coordination and a very low redox potential around −260 mV (for review see Ref. 2). Shen *et al.* (3–5) showed that cyt c_{550} is stoichiometrically bound to the Photosystem II (PS II), activates oxygen evolving activity and allows the binding of the 12 kDa protein, another extrinsic component of the cyanobacterial PS II involved in oxygen evolution. The three-dimensional structure of the PS II from two thermophilic cyanobacteria strains confirmed that cyt c_{550} binds to the luminal PS II surface in the vicinity of the D1 and CP43 proteins (6–8). The phenotype of the ΔpsbV (cyt c_{550}-less) mutant of *Synechocystis* PCC 6803 was already characterized with respect to PS II activity (9–11). The ΔpsbV and the double ΔpsbV/ΔpsbU (encoding the 12 kDa protein) mutants were unable to grow in the absence of Ca^{2+} and Cl^- ions, their PS II activity decreased to 40% of the wild type, and they showed a very rapid inactivation of the enzyme in the dark (after 2 h, the activity decreased about 90% whereas in the wild type only 25% of the activity was lost). A slight retardation in O_2 release from the S_3 state was also observed in these mutants. Another effect observed in these *Synechocystis* PCC 6803 mutants was a large intensity decrease of the B band of thermoluminescence (TL) and an upshift in the temperature maxima of the B and Q bands. The upshift of the TL bands was attributed to the lack of the 12 kDa protein, and the decrease in the intensity of the B band was considered to be the major effect of cyt c_{550} deletion (11). All these observations led the authors to propose that cyt c_{550} functions in maintaining the high affinity of PS II for Ca^{2+} and Cl^- and in protecting the Mn-cluster from attack by bulk reductants (9–11).

The low midpoint redox potential (E'_m) values of the purified cyt c_{550} (from −250 to −314 mV (1, 12, 13)) seems incompatible with a redox function in PS II electron transfer. However, we have recently demonstrated that the cyt c_{550} from the thermophilic cyanobacteria *Thermosynechococcus elongatus* has a significantly higher E'_m value when it is bound to the PS II (−80/−100 mV) compared with its soluble form after its extraction from PS II (−240 mV at pH 6) (14). Moreover, while the E'_m of the bound form is pH-independent, the E'_m of the soluble form varies from −50 mV at pH 4.5 to −350 mV at pH 9–10 (14). In conditions more native than isolated PS II complexes, it is possible that the E'_m of cyt c_{550} may be even higher than −80/−100 mV, and thus a redox function in the water oxidation complex could be conceivable.

The thermophilic cyanobacterium *T. elongatus* has become a new model organism for photosynthesis research since it has provided the first resolved x-ray crystallographic structures of PS I (15) and PS II (6). As mentioned above, cyt c_{550} is encoded by the *psbV* gene, however in the thermophilic strains *T. elongatus* and *T. vulcanus*, the genome contains a second gene (*psbV2*) encoding a cyt c_{550}-like protein located between the *psbV1* gene (encoding cyt c_{550}) and the *petJ* gene (encoding cyt c_6, soluble electron donor of PS I) (16). We have recently shown

* The costs of publication of this article were defrayed in part by the payment of page charges. This article must therefore be hereby marked "*advertisement*" in accordance with 18 U.S.C. Section 1734 solely to indicate this fact.

§ To whom correspondence should be addressed. Tel.: 33-1-69-08-95-71; Fax: 33-1-69-08-87-17; E-mail: diana.kirilovsky@cea.fr.

[1] The abbreviations used are: cyt c_{550}, cytochrome c_{550}; PS II, Photosystem II; Chl, chlorophyll; E'_m, midpoint redox potential; EPR, electron paramagnetic resonance; PS I, photosystem I; Sp, spectinomycin; Sm, streptinomycin; MES, 2-(*N*-morpholino) ethanesulfonic acid; DCBQ, 2,6 dichloro-p-benzoquinone; TL, thermoluminescence; Tricine, *N*-[2-hydroxy-1,1-bis(hydroxymethyl)ethyl]glycine.

that this gene is expressed (17). The PsbV2 protein has an apparent molecular mass of about 15.3 kDa and contains a six-coordinated low spin *c*-type heme, and the sixth ligand seems to be the Tyr-86. The role of the PsbV2 protein is unknown.

The present study is an attempt to analyze the possible role of the heme of the cyt c_{550} in PS II. To address this problem, two mutants of the thermophilic cyanobacterium *T. elongatus* were constructed. In these mutants, the His-92, the sixth ligand of the heme, was changed to a methionine or cysteine to modify the redox properties of the heme. In addition, in these two mutants, the *psbV2* gene was disrupted by an antibiotic cassette in order to allow its selection. Two other mutants were constructed and studied here: a *psbV2*-disruptant mutant (ΔpsbV2) as a control strain, and a *psbV1*-disruptant mutant (ΔpsbV1 or cyt c_{550}-less mutant).

EXPERIMENTAL PROCEDURES

Strain and Standard Culture Conditions—Cells of the transformed strain of *T. elongatus* with a histidine tag on the CP43 protein of PS II (43-H strain) (18) and all the other mutants constructed for this work were grown in a rotary shaker (120 rpm) at 45 °C under continuous illumination from fluorescent white lamps giving an intensity of about 80 μmol of photons m^{-2} s^{-1}. Cells were grown in a DTN medium (19) in a CO_2-enriched atmosphere. For maintenance, the cells were grown in the presence of kanamycin (40 μg ml^{-1}) or spectinomycin (25 μg ml^{-1})/streptomycin (10 μg ml^{-1}). For PS II preparations, the cells were grown in 3-liter conical flasks (1500 ml of culture). For Ca^{2+} depletion, in the DTN medium, $CaCl_2$ was replaced by NaCl. For Cl^- depletion, $CaCl_2$, $FeCl_3$, and NH_4Cl were replaced by $CaOH_2$, $FeNH_4(SO_4)_2$, $(NH_4)_2SO_4$, respectively.

Cloning, Recombinant Plasmids, and in Vitro Mutagenesis—The genome region containing the *psbV1* and *psbV2* genes was amplified using genomic DNA of *T. elongatus* as template and two synthesized oligonucleotides: psV1, 5′-CGCGGATCCACATGAACAGTGTACGCTGT-3′ and psV2, 5′-CCGGAATTCAACGGAGTTCTCCTTTCAT-3′, containing the BamHI and EcoRI restriction sites, respectively, were used as primers. The amplified region of 1.5 kb containing the *psbV1*, *psbV2* genes and the flanking regions was first cloned in the polylinker EcoRV restriction site of a pBC-SK^+ chloramphenicol-resistant plasmid (dpV1 plasmid) and then in the BamHI restriction site of a pUC9 ampicillin-resistant plasmid (dpV2 plasmid).

Insertional inactivation of the *psbV2* gene was carried out by inserting a 2.2-kb DNA fragment containing the *aadA* gene from Tn7, conferring resistance to spectinomycin and streptinomycin (Sp/Sm) (20), in the unique BstAPI restriction site of the *psbV2* gene in the dpV1 plasmid (dpV3 plasmid). Insertional inactivation of the *psbV1* gene was achieved with the insertion of the Sp/Sm cassette in the unique BsaAI restriction site of *psbV1* in the dpV2 plasmid (dpV4 plasmid).

Site-directed mutagenesis of the plasmid containing the interrupted *psbV2* gene (dpV3 plasmid) was performed using the QuikChange XL site-directed mutagenesis kit of Stratagene as recommended by the manufacturer. Synthetic mutagenic oligonucleotides: 5′-GAAATTGCTGAGGTGATGCCCAGTCTGCGCAGT-3′ and 5′-GAAATTGCTGAGGTGTGCCCCAGTCTGCGCAGT-3′ were used to create in the *psbV1* gene the H92M and H92C mutants, respectively. These primers delete the unique ApaLI restriction site of the *psbV1* gene.

Transformation of T. elongatus Cells and Genetic Analysis of Mutants—The plasmids containing the interrupted genes and the site-mutated genes were introduced in 43-H *T. elongatus* cells by electroporation according to Ref. 19 with slight modifications. After washing once with 2 mM Tricine, 2 mM EDTA, and twice with double-distilled water, the cells were resuspended at an OD_{750} of about 100 (approx 1×10^{11} cells ml^{-1}). 40 μl of this suspension was mixed with 4–8 μl of a 0.5–1 μg μl^{-1} DNA and chilled on ice. Cells were electroporated in chilled, sterile cuvettes with a 2 mm gap between the electrodes with a single pulse with a time constant of 5 ms and at field strength of 9 kV/cm. After electroporation, cells were rapidly transferred to 2 ml of DTN and incubated for 48 h in a rotary incubator at 45 °C under low light conditions. Then, the cells in 0.1–0.2 ml aliquots were spread on Sp/Sm-containing plates (12 μg ml^{-1}/6 μg ml^{-1}) and incubated at 45 °C, under dim light and humidified atmosphere. Once transformants emerged as green colonies after 2–3 weeks, they were spread at least twice on agar plates containing 25 μg ml^{-1} spectinomycin and 10 μg ml^{-1} streptinomycin before their genomic DNA was analyzed.

Genomic DNA was isolated from *T. elongatus* cells essentially as described by Cai and Wolk (21). To confirm the homoplasmicity of the Δ*psbV2* and Δ*psbV1* mutants a PCR analysis was carried out using primers psV1 and psV2. To verify that the desired point mutations were present in the transformed *T. elongatus* cells, a PCR fragment containing the *psbV1* gene was obtained using the oligonucleotides psV0, 5′-TCCGGCACCGCCCCCAAGGATAAT-3′ and psV6, 5′-CCGGCGCGATCGTCCAGCCCAGCA-3′. The amplified fragment was then digested by the restriction enzyme ApaLI. The mutant PCR fragments were then sequenced to confirm that the correct mutation was the only modification present in the gene.

Thylakoids and PS II Core Complexes Preparation—Thylakoids and PS II core complexes were prepared as described by Roncel *et al.* (14) with the following modifications: 1) All the buffers used in the preparations contained 1 M glycinebetaine and 10% (v/v) glycerol. 2) The supernatant of the β-D-dodecyl-maltoside treated thylakoids was mixed with 1 volume of Probond™ resin (Invitrogen, Groningen, The Netherlands) and immediately transferred to an empty column and washed. 3) The PS II preparations were resuspended in 40 mM MES, pH 6.5, 15 mM $MgCl_2$, 15 mM $CaCl_2$, 10% (v/v) glycerol, and 1 M glycinebetaine at about 2 mg of Chl·ml^{-1}. The preparations used in this work had an oxygen evolution activity of 2200–3000 μmol of O_2·mg Chl^{-1}·h^{-1}.

Cytochrome c_{550} Isolation—Cyt c_{550} from the ΔpsbV2 mutant was isolated from soluble proteins as described in Ref. 17 and from PS II preparations as described in Ref. 23. Cyt c_{550} from H92M and H92C mutants were isolated only from PS II preparations. Incubation of isolated PS II complexes in a solution of 20 mM MES, pH 6.5 containing 10 mM sodium ascorbate for 1 h (4 °C) under daylight induced the release of the cyt c_{550} from the PS II. The PS II cores were precipitated by centrifugation (170,000 × *g*, overnight). The supernatant containing the 33 kDa protein, the 12 kDa protein, and the cyt c_{550} was concentrated, and then the cyt c_{550} was purified by HPLC on a Hi-Trap Q Sepharose HP column (Hepes 10 mM, pH 7, sodium ascorbate 10 mM, 0–1 M NaCl gradient).

Oxygen Evolution Measurements—Oxygen evolution was measured at 25 °C by polarography using a Clark-type oxygen electrode with saturating white light. Oxygen evolution of cells (20 μg of Chl ml^{-1}), thylakoid membranes (20 μg of Chl ml^{-1}), and PSII core complexes (5 μg of Chl ml^{-1}) was measured in 40 mM MES, pH 6.5, 15 mM $MgCl_2$,15 mM $CaCl_2$, 10% (v/v) glycerol, 1 M glycinebetaine, and in the presence of 0.5 mM DCBQ (2,6-dichloro-*p*-benzoquinone, dissolved in ethanol) as electron acceptor. The amount of oxygen produced per flash during a sequence of saturating flashes was measured at room temperature with a lab-made rate electrode equivalent to that described in (22). The short saturating flashes were produced by a xenon flash. The time between flashes was 400 ms. 20 μl of a thylakoid membrane suspension (1 mg of Chl·ml^{-1}) in a buffer containing 40 mM MES, pH 6.5, 15 mM $MgCl_2$, 15 mM $CaCl_2$, 10% (v/v) glycerol, 1 M glycinebetaine were deposited onto the surface of the platinum electrode and dark adapted for 40 min at room temperature prior to each flash sequence. The analysis of the flash-induced oxygen evolution patterns was done as described in Ref. 23.

EPR Measurements—CW-EPR spectra were recorded using a standard ER 4102 (Bruker) X-band resonator with a Bruker ESP300 X-band spectrometer equipped with an Oxford Instruments cryostat (ESR 900). The samples were frozen in the dark to 198 K, degassed at 198 K, and then transferred to 77 K. Determination of *g*-values was done using an ER032M gaussmeter (Bruker). Illumination of the samples was done with an 800 watt tungsten lamp, in a non-silvered Dewar filled with liquid nitrogen. Light was filtered through water and IR filters.

To calculate the PS II/PS I ratio, first an EPR spectrum of Tyr $D^{\bullet}$ was recorded using a dark-adapted sample. A second EPR spectrum was recorded after one flash in the presence of ferricyanide (in order to oxidize all the Tyr D and the $P700^+$). Then the Tyr $D^{\bullet}$ signal was removed from the spectrum by interactive subtraction to obtain the P700 and Tyr $D^{\bullet}$ signals separately. Interactive subtraction is a standard computer-assisted spectrum manipulation in which an unknown spectral component can be extracted from a mixture of two spectra by subtracting a proportion of a second known spectral component. The proportion of the known spectral component in the mixture is gradually varied until the difference spectrum is considered to contain no contribution from the known spectrum.

Redox Potential Measurements—Reductive Potentiometric redox titrations were carried out basically as described in Ref. 14. The electrode was calibrated before each titration against a saturated solution of quinhydrone (E'_m = +280 mV at 20 °C, pH 7). All redox measurements are relative to normal hydrogen electrode. For titration, samples contained PS II core complexes (30–50 μg of Chl ml^{-1})

or purified cyt c_{550} (about 0.5–1 μM) were suspended in a buffer containing 40 mM MES, pH 6.5, 15 mM $MgCl_2$, 15 mM $CaCl_2$, 10% (v/v) glycerol, and 1 M glycinebetaine. The buffer for the titrations of purified H92C and H92M cyt c_{550} contained 10 mM sodium ascorbate. To ensure a good equilibrium between the redox centers and the electrode, a set of suitable redox mediators were added (14):20 μM duroquinone (E'_m, pH 7 = +10 mV), 30 μM 2-methyl-1,4-naphthoquinone (E'_m, pH 7 = 0 mV), 30 μM 2,5-dihydroxyl-*p*-naphthoquinone (E'_m, pH 7 = −60 mV), 30 μM anthraquinone (E'_m, pH 7 = −100 mV), 30 μM 2-hydroxyl-1,4-naphthoquinone (E'_m, pH 7 = −145 mV), 30 μM anthraquinone-1,5-disulfonate (E'_m, pH 7 = −170 mV), 30 μM anthraquinone-2,6-disulfonate (E'_m, pH 7 = −185 mV) and 30 μM anthraquinone-2-sulfonate (E'_m, pH 7 = −225 mV), 30 μM benzyl viologen (1,1′-dibenzyl-4,4′-bipyridylium dichloride) (E'_m, pH 7 = −311 mV) and 30 μM methyl viologen (1,1′-dimethyl-4,4′-bipyridylium dichloride) (E'_m, pH 7 = −430 mV). In order to calculate E'_m values of cyt c_{550} in PSII core complexes, differential spectra were obtained by subtracting the absolute spectra recorded at each solution redox potential during titrations from the spectra of the fully oxidized state of the cytochrome (at a solution redox potential of about +100 mV). The absorbance differences at 549–560 nm (for ΔpsbV2 mutant) and 552–560 nm (for His-92 mutants) obtained from difference (PSII core complexes) or absolute spectra (purified cyt c_{550}) were normally converted into percentages of reduced cytochrome and plotted *versus* solution redox potential. E'_m values were then determined by fitting percentages plots to an $n = 1$ Nernst equation curve using a nonlinear curve-fitting program (Origin 6.0, Microcal Software). Oxidative redox titrations were carried out as controls in order to check for the reproducibility of the experiments; no significant hysteresis effects were observed.

Thermoluminescence—Thermoluminescence was measured as described in (24). Thylakoid membranes at a Chl concentration of 100 μg ml^{-1} and PS II complexes at 35 μg ml^{-1} were dark-adapted (at least for half an hour). Cells were centrifuged and resuspended in a 40 mM MES (pH 6.5) buffer containing 15 mM MgCl, 15 mM CaCl, 10% glycerol, and 1 M glycinebetaine at a Chl concentration of 100 μg ml^{-1}. After dark adaptation (15 min), the cells were frozen at −80 °C. They were maintained for half an hour at −80 °C. After slow thawing, the cell suspension was incubated on ice in darkness. For measurements of $S_2Q_B^-$ and $S_3Q_B^-$ recombination, the samples were incubated for 5 min in the dark at 20 (isolated PS II) or 40 °C (thylakoids and cells) and then flashed one to four times at 1 °C. For measurements of $S_2Q_A^-$ recombination, the dark-adapted samples were flashed once in the presence of DCMU at 20 °C and after 3 min of dark adaptation, one flash was given at −5 °C. For luminescence detection, the samples were warmed at a constant rate (0.5 °C/s) from 1 °C or −5 °C to 80 °C.

RESULTS

Construction of Gene-interrupted and Site-directed Mutants—To generate mutants of *T. elongatus* lacking either the cyt c_{550} or the PsbV2 protein, the genome region containing the genes coding for these proteins (Fig. 1*A*) was amplified by PCR and cloned. Plasmids were constructed in which either the *psbV1* or the *psbV2* gene was interrupted by insertion of a spectinomycin/streptomycin resistance cassette (Fig. 1, *B* and *C*). The plasmids carrying the site-directed mutations H92M-*psbV1* and H92C-*psbV1* were constructed using the plasmid in which the *psbV2* gene had been previously interrupted. Thus, the PsbV2 protein was absent in these mutants. The plasmids were introduced into H-43 *T. elongatus* cells by electroporation and the interrupted *psbV2* and point-mutated *psbV1* genes were incorporated into the cyanobacterium genome by homologous double recombination.

The construction allowed us to perform mutant selection by growing the cells in the presence of antibiotics. Complete segregation and homoplasmicity of the mutants were tested by PCR analysis. Fig 1*E* shows that amplification of the genomic region containing the *psbV1* and *psbV2* genes using the synthetic oligonucleotides psV1 and psV2 gave a fragment of 3.5 kb in all the mutants containing the Sp/Sm cassette (2.1 kb) instead of a 1.5 kb fragment as was observed in the H-43j *T. elongatus* strain. No traces of the 1.5 kb PCR fragment were detected in these mutants indicating that complete segregation and total homoplasmicity were achieved in mutant cells. The digestion pattern obtained with the restriction enzyme ApaLI of the 3.5-kb fragment confirmed that the Sp/Sm resistance cassette was incorporated in the BsaAI site of the *psbV1* gene in the *psbV1*-disruptant mutant and in the BstAPI site of *psbV2* in the *psbV2*-disruptant mutant (Fig. 1, *D* and *F*).

Since the double recombination could occur between the antibiotic cassette and the point mutations, not all the Sp/Sm resistant mutants contained the site-directed mutations. To select the mutants carrying the proper modified bases, a 1-kb PCR fragment obtained using the psV0 and psV6 oligonucleotides as primers and containing the *psbV1* gene was checked by digestion with the restriction enzyme ApaLI. In the absence of a point mutation, the fragment was digested giving two fragments of 0.8 and 0.2 kb (Fig. 1*G*). The smaller fragment is visible only on overloaded gels (data not shown). With the correct mutation, the amplified DNA fragments lost the restriction site, and no digestion occurred (Fig. 1*G*). Sequencing of the PCR-amplified fragment confirmed the presence of the proper mutation (data not shown). These PCR analyses were regularly repeated to verify the genotype in the cells used for phenotype characterization.

For simplicity, the *psbV2*-disruptant mutant, lacking the PsbV2 protein, but presenting a phenotype similar to the wild type is called the control strain; the *psbV1*-disruptant mutant, lacking the cyt c_{550}, is called the cyt c_{550}-less mutant; the Δ*psbV2*/H92M-*psbV1* and Δ*psbV2*/H92C-*psbV1* mutants is called H92M and H92C, respectively.

Mutant Cell Growth—The photosynthetic growth rates of control cells and H92M, H92C, and cyt c_{550}-less mutant cells at 45 °C and 80 μmol of photons m^{-2} s^{-1} were similar (Fig. 2*A*). The doubling time was about 20 h for the four strains. The *T. elongatus* cyt c_{550}-less mutant cells were unable to grow in DTN medium lacking Cl^- (Fig. 2*B*). Control, H92M, and H92C cells, however, were able to grow in the chloride-depleted culture medium albeit at slower rate (doubling time ≈35–37 h). In Ca^{2+}-depleted medium, *T. elongatus* wild type cells only doubled their initial concentration before they completely stopped growing (Fig. 2*B* and Ref. 27). The control, H92M and H92C cells presented the same behavior as the wild type cells whereas cyt c_{550}-less mutant cells did not grow at all (Fig. 2*B*).

Oxygen Evolution Activity—The H92M, H92C, and control cells had similar oxygen evolving activities (250–300 μmol of O_2·(mg Chl)$^{-1}$·h^{-1}) while the activity was significantly lower in the cyt c_{550}-less mutant cells (150–200 μmol of O_2·(mg Chl)$^{-1}$·h^{-1}). We measured the oxygen evolution activity under different light intensities in control and cyt c_{550}-less mutant cells. By plotting the data as the activity *versus* activity/light intensity (Fig. 3) (25–27), straight parallel lines were obtained indicating that the number of active PS II reaction centers decreased in cyt c_{550}-less mutant cells compared with control cells. EPR measurements (see "Experimental Procedures") indicated that the ratio PS I to total PS II was about 2.5–3 in the four strains (data not shown).

The oxygen-evolving activity in H92M and control thylakoids was similar to that measured in whole cells (240–270 μmol O_2·(mg Chl)$^{-1}$·h^{-1}), while in cyt c_{550}-less and H92C thylakoids the activity decreased to 160–200 and 100–130 μmol of O_2·(mg Chl)$^{-1}$·h^{-1}, respectively. Thus, the activity of H92C thylakoids represented 60–75% of the activity of control thylakoids, and the activity of cyt c_{550}-less thylakoids was only 40–48% of control.

Highly active PS II complexes (2700–3000 μmol of O_2·(mg Chl)$^{-1}$·h^{-1}) were isolated from control cells as described in Roncel *et al.* (14). With this method, the PS II complexes isolated from H92M and H92C mutants had much lower activities

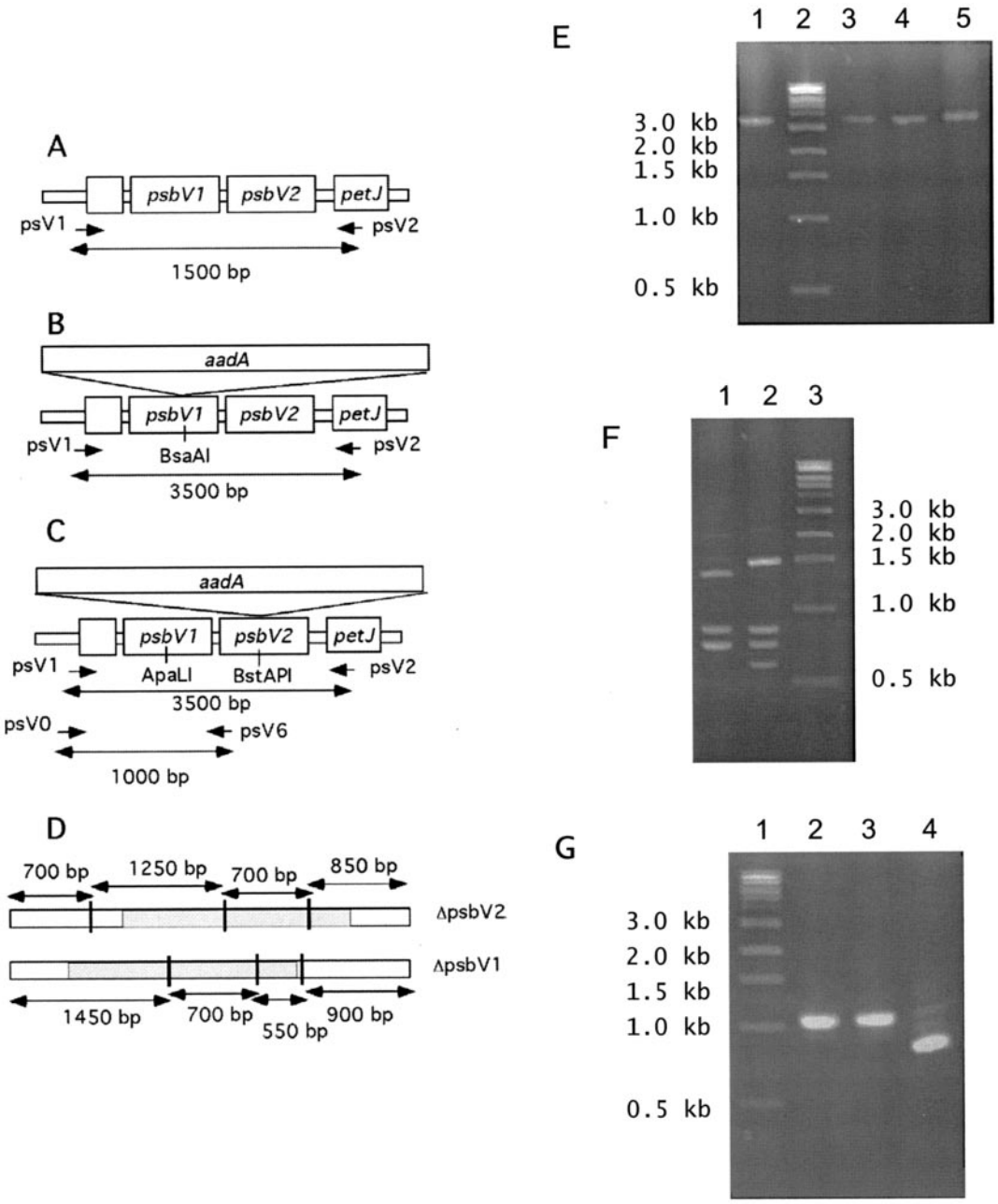

FIG. 1. **Mutant construction and test for the presence of mutations.** *A*, gene arrangement of the *psbV1* and *psbV2* genes and flanking regions. The primers used in PCR amplification are indicated (*B* and *C*) *psbV1* or *psbV2* gene disruption by insertion of the Sp/Sm resistance cassette (*aadA*) in the BsaAI site in the *psbV1* gene and in the BstAPI site in the *psbV2* gene. *D*, size of fragments that must be obtained by digestion with the restriction enzyme ApaLI of the 3.5 kb-amplified PCR fragment of genomic *T. elongatus* ΔpsbV1 and ΔpsbV2 mutants using as primers the psV1 and psV2 oligonucleotides. *E*, amplification of genomic DNA from ΔpsbV2 (*lane 1*), ΔpsbV1 (*lane 3*), H92M (*lane 4*), and H92C mutants using as primers psV1 and psV2 oligonucleotides. *F*, digestion by ApaLI of the 3.5 kb-amplified PCR fragments obtained using as template ΔpsbV2 (*lane 1*) and ΔpsbV1 (*lane 2*) DNAs. *G*, digestion by ApaLI of the 1-kb PCR fragments obtained using as templates H92M (*lane 2*), H92C (*lane 3*), and ΔpsbV2 DNAs.

(500–800 μmol of O_2·(mg Chl)$^{-1}$·h^{-1}). We observed that during the purification, the cyt c_{550} and the 12 kDa protein were completely lost from the PS II complexes (data not shown). PS II complexes with higher activities were obtained from both mutants when the isolation was done using 1 M glycinebetaine in all the buffers. Glycinebetaine is an osmoprotective plant product known for its stabilizing properties of the oxygen-evolving complex (28, 29). Even in the presence of glycinebetaine, the PS II complexes from the mutants were less active than the control PS II complexes: the H92C PS II complexes (1900–2300 μmol of O_2·(mg Chl)$^{-1}$·h^{-1}) were systematically less active than the H92M PS II complexes (2500–2800 μmol of O_2·(mg Chl)$^{-1}$·h^{-1}). The lower activity in isolated PS II from H92C seemed to correspond to a lower amount of cyt c_{550} associated with the PS II complex. In Fig. 4 the difference spectra of cyt c_{550} and cyt b_{559} shows that quantity of cyt c_{550} present in isolated PS II complexes was as follows: control > H92M >H92C mutants. Fig. 4, *B* and *C* also show that the mutations induced an upshift from 549 to 552 nm of the maxima of the α band in the bound and unbound cyt c_{550}.

Illumination of dark-adapted samples by a train of short saturating flashes produces oxygen with a yield per flash that oscillates with a periodicity of four (30, 31). Fig. 5, *A* and *B* show the oxygen emission under flash illumination in thylakoids isolated

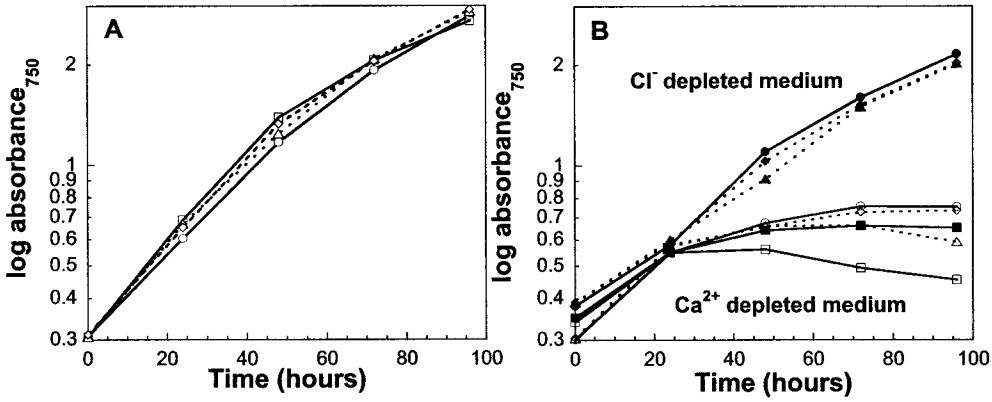

FIG. 2. **Growth curves.** Growth curves of control (ΔpsbV2) (*circles*), cyt c_{550}-less mutant (ΔpsbV1) (*squares*), H92C mutant (*triangles*), and H92M mutant (*rhomboids*) cells in complete medium (*A*) or without Ca^{2+} (*B*, *open symbols*) or Cl^- (*B*, *closed symbols*). Temperature of growth: 45 °C.

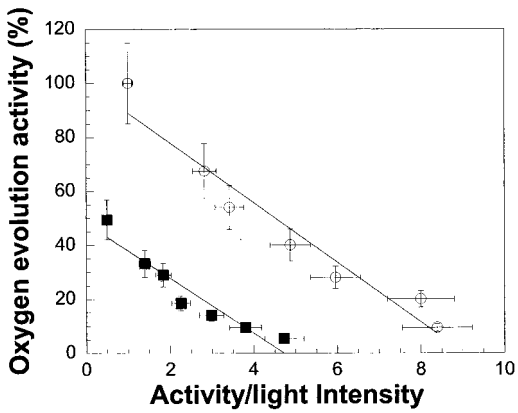

FIG. 3. **Oxygen-evolving activity as function of activity/light intensity of control (*squares*) and cyt c_{550}-less mutant (*circles*) cells (20 μg of Chl/ml) in the presence of 0.5 mM DCBQ.**

from the four strains. The oscillation was pronounced and clear maxima were observed after the third, seventh, and eleventh flashes (Fig. 5, *A* and *B*). The pattern of the oscillations (Fig. 5, *A* and *B*), the miss parameter, and the initial S_0 and S_1 values in control and H92M and H92C mutants were similar (S_0 = 10–15%; S_1 = 85–90%; α = 0.09–0.12). In cyt c_{550}-less mutant thylakoids, the amplitude of oscillations was smaller and the dark concentration of S_0 was higher (25–27% *versus* 10–15%) than in the other strains (Fig. 5*A*).

In order to examine whether the absence of the cyt c_{550} retarded the oxygen release from the S_3 state, we measured the kinetics of oxygen release after the third flash (Fig. 5*C*). The peak of the oxygen signal for the cyt c_{550}-less mutant reproducibly located 1–2 ms later than that for the control (7 *versus* 5 ms) (Fig. 5*C*). The $t_{1/2}$ for the oxygen release was estimated to be 1.5 ms in the control thylakoids and 2 ms in cyt c_{550}-less mutant thylakoids. His-92 mutations did not change the kinetics of oxygen release (data not shown).

Characteristics of the Cyt c_{550} from control and H92M and H92C Mutants—The cyt c_{550} of control cells was isolated 1) from the fraction of soluble proteins and 2) from isolated PS II complexes. The N-terminal amino acid sequence of the cyt c_{550} from both sources was AELTPE. This result indicates that the cyt c_{550} from both origins had lost the 26 amino acids transit sequence. Moreover, the absorbance spectra and redox properties of cyt c_{550} from both sources were identical (data not shown).

Cyt c_{550} from the H92C and H92M mutants was isolated only from isolated PS II complexes. Although the cyt c_{550} was present in the cytoplasm/periplasm fraction of these mutants, it was not possible to isolate it from this fraction. It seemed to be degraded during the different steps of purification. The presence of sodium ascorbate (used as an antioxidant) decreased the rate of denaturation of the mutant cytochromes. However, the H92M cyt c_{550} was so unstable that it began to be denaturated during the final step of purification (HPLC) even in the presence of sodium ascorbate. The absorbance spectrum, redox potential measurements and EPR spectra indicated that during the HPLC purification the methionine was lost as the sixth ligand (data not shown). All the data concerning the H92M cyt c_{550} shown in this article were obtained without HPLC purification.

The redox properties of wild-type cyt c_{550} of *T. elongatus* have been already described in a previous article (14). Fig. 6 shows reductive potentiometric titrations at pH 6.5 of the cyt c_{550} of the control and of the H92M and H92C mutants when bound to PS II (*closed symbols*) and in its soluble form (*open symbols*). In control cells, the E'_m of the bound cytochrome was significantly higher than that of the cytochrome in solution (−110 ± 8 mV *versus* −265 ± 11 mV). The E'_m of the isolated cytochrome was pH-dependent (pH 6: E'_m = −224 mV, pH 7: E'_m = −286 mV, data not shown) like in the wild type (23). The mutation of the His to Cys decreased the redox potential of the soluble cyt c_{550} to about −300 ± 7 mV (Fig. 6). The E'_m of the bound H92C cyt c_{550} was significantly higher (−164 ± 9 mV) than that of the unbound cytochrome (Fig. 6). In contrast, the isolated H92M cyt c_{550} and the bound H92M cyt c_{550} had similar redox potentials of about −140 ± 10 mV. Thus, the mutation His to Met induced a significant increase of the redox potential of the isolated cyt c_{550}, and the loss of the binding effect on the redox potential.

EPR Spectra of Cyt c_{550} in Control and H92M and H92C Mutants—EPR spectra of PS II-bound and isolated cyt c_{550} are reported in Fig. 7, *panels A* and *B*, respectively. In *panel A*, spectrum *a* was recorded on control-PS II. In principle, spectrum *a* could contain both cyt b_{559} and cyt c_{550} signals. However, in intact PSII, cyt b_{559} is mainly in a reduced state in darkness and thus EPR-silent, whereas cyt c_{550} is oxidized and thus detectable by EPR (14). The g_z (3.02), g_y (2.21), and g_x (1.44) values of cyt c_{550} were similar to those found earlier in the wild type (14). These values are characteristic of a bis-histidine hexa-coordinated low spin heme with a rhombicity of 0.48 (14, 17). Spectra *b* and *c* were recorded on H92C and H92M PS II mutants, respectively. In both samples, two distinct g_z and g_y resonances contribute to the spectra (the broadness of the g_x resonances makes them more difficult to detect). This suggests either a heterogeneity in the cyt c_{550} or the presence of a second oxidized cytochrome. The values of g_z resonances at 3.02 and that of the g_y resonances at ~2.2 suggest that the

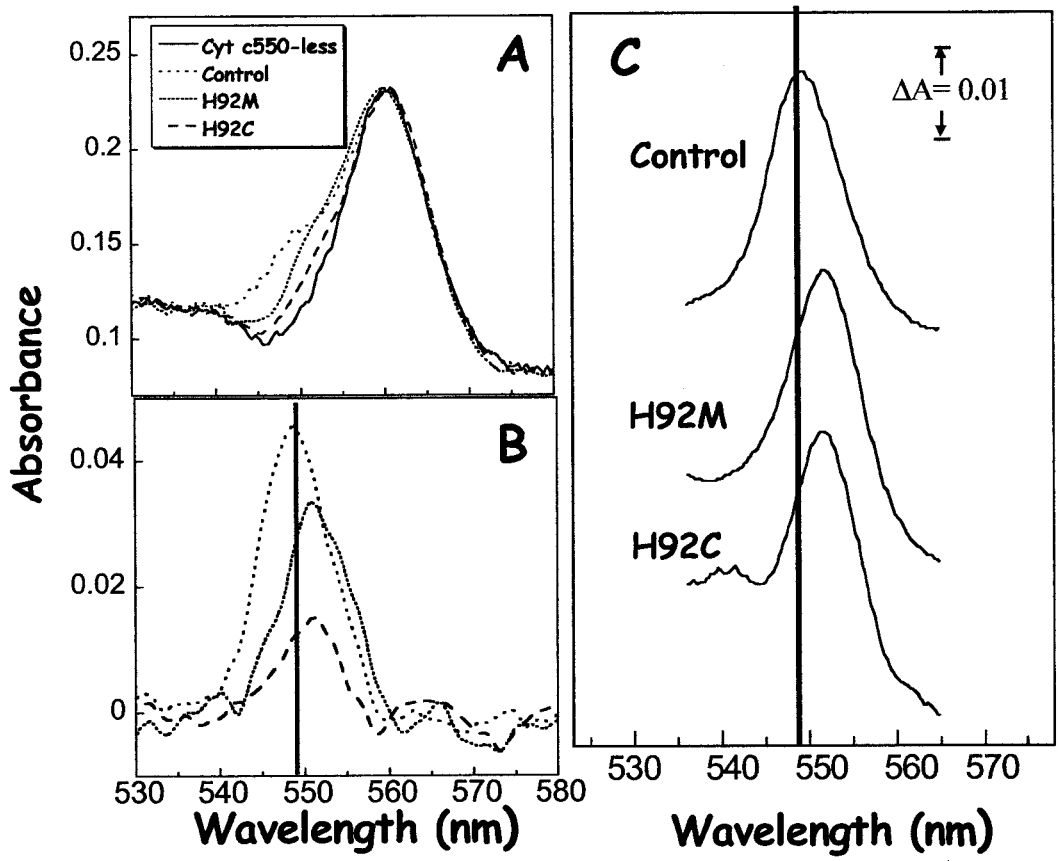

FIG. 4. *A*, redox difference absorption spectra of the cytochromes b_{559} and c_{550} in PS II-isolated complexes from *T. elongatus* ΔpsbV2 (control), ΔpsbV1 (cyt *c550*-less), H92M, and H92C strains. The spectra were obtained by subtracting absolute spectra recorded at −300 mV minus at +458 mV. *B*, spectra of bound cyt c_{550} in PS II-isolated complexes *T. elongatus* ΔpsbV2 (control), H92M, and H92C strains. The spectra were obtained by subtracting the spectra of cyt c_{550} and b_{559} of the cyt c_{550}-less mutant (shown in *A*) to those of the other three strains. *C*, α band of reduced soluble cyt c_{550} isolated from control and H92M and H92C mutants.

minor contributions in both spectra *b* and *c* originated from the relaxed high potential form of ferri-cyt b_{559} in a fraction of the centers (32). The g_z (2.91), g_y (2.27), and g_x (1.55) resonances are similar in both the H92C and H92M PSII mutants. These values indicate a rhombicity of 0.59 and a tetragonality of 3.36, which correspond to hexa-coordinated low spin heme close to the domain characteristic of thiolate heme ligands in the Peisach and Blumberg diagram (33).

Panel B in Fig. 7 shows the EPR spectra of cyt *c550* isolated from control-PS II (*spectrum a*), from H92C-PS II (*spectrum b*) and H92M-PS II (*spectrum c*). Cyt c_{550} isolated from control-PS II has the EPR characteristics previously reported (14, 17) with g_z = 2.97, g_y = 2.24, and g_x = 1.49. In the isolated H92C cytochrome the *g*-values were g_z = 2.94, g_y = 2.26, and g_x = 1.53 and in the isolated H92M cytochrome the *g*-values were g_z = 2.92, g_y = 2.27, and g_x = 1.54. Spectra b and c also contain traces of contaminating MnII, which exhibits a 6-line spectrum between ≈3100 and ≈3800 gauss. In the isolated cytochromes from both the H92C and H92M mutants the rhombicity (0.56–0.58) and the tetragonality (3.3–3.4) values are similar to those found in the bound cytochromes. This strongly differs from the situation encountered in the wild type, where the rhombocity value in the isolated cytochrome (0.58) was higher than that in the PS II-bound cytochrome (0.48) (14, 17).

Fig. 8 shows the EPR spectra of wild-type cyt c_{550} recorded using: (*a*) the purified cytochrome isolated from cells, (*b*) whole cells, (*c*) purified thylakoids, (*d*) purified PSII. The g_z value of the thylakoid-bound cyt c_{550} corresponded to that of PS II-bound cyt c_{550} and that of the whole cells to that of the isolated cyt c_{550} with a shoulder that could be from the bound cyt c_{550}. These results suggest the presence of a significant concentration of soluble cyt c_{550} in control cells. Comparing the quantity of the cyt c_{550} isolated from soluble fraction of 20 liters of cells to the number of PS II present in these cells, we calculated that the soluble fraction could represent between 40 and 60% of the bound population. In His-92 mutant cells the EPR signals from cyt c_{550} were very weak but the g_z values seemed to correspond better to those of the PS II-bound cytochrome rather than to those of isolated cyt c_{550} (data not shown), supporting the idea that the mutant cytochromes are unstable in their soluble form.

Thermoluminescence Studies of T. elongatus Mutants—In this section, we will describe the characteristics of the thermoluminescence bands in whole cells, thylakoids and isolated PS II complexes of the four mutants of *T. elongatus* that were studied. The thermoluminescence (TL) emitted at physiological temperatures arises from charge recombination from $S_{2/3}$ with Q_B^- (the Q band) and from $S_{2/3}$ with Q_B^- (the B band) (34, 35). The TL pattern of unfrozen cells was variable due to different values of the dark stable transmembrane proton (and/or electrochemical) gradient, which induces a temperature downshift of the B bands (36), which changed from one culture batch to another. Thus, the comparison between the mutants was done using cells that had been frozen and thawed, a treatment that collapses the transmembrane proton gradient. In these treated cells the pattern of TL was stable, independent of the cell batch and similar to that obtained with cells treated with the protonophore nigericin (data not shown).

Fig. 9*A* compares the oscillation of the B band intensity in the frozen and thawed cells after a series of flashes. The B band

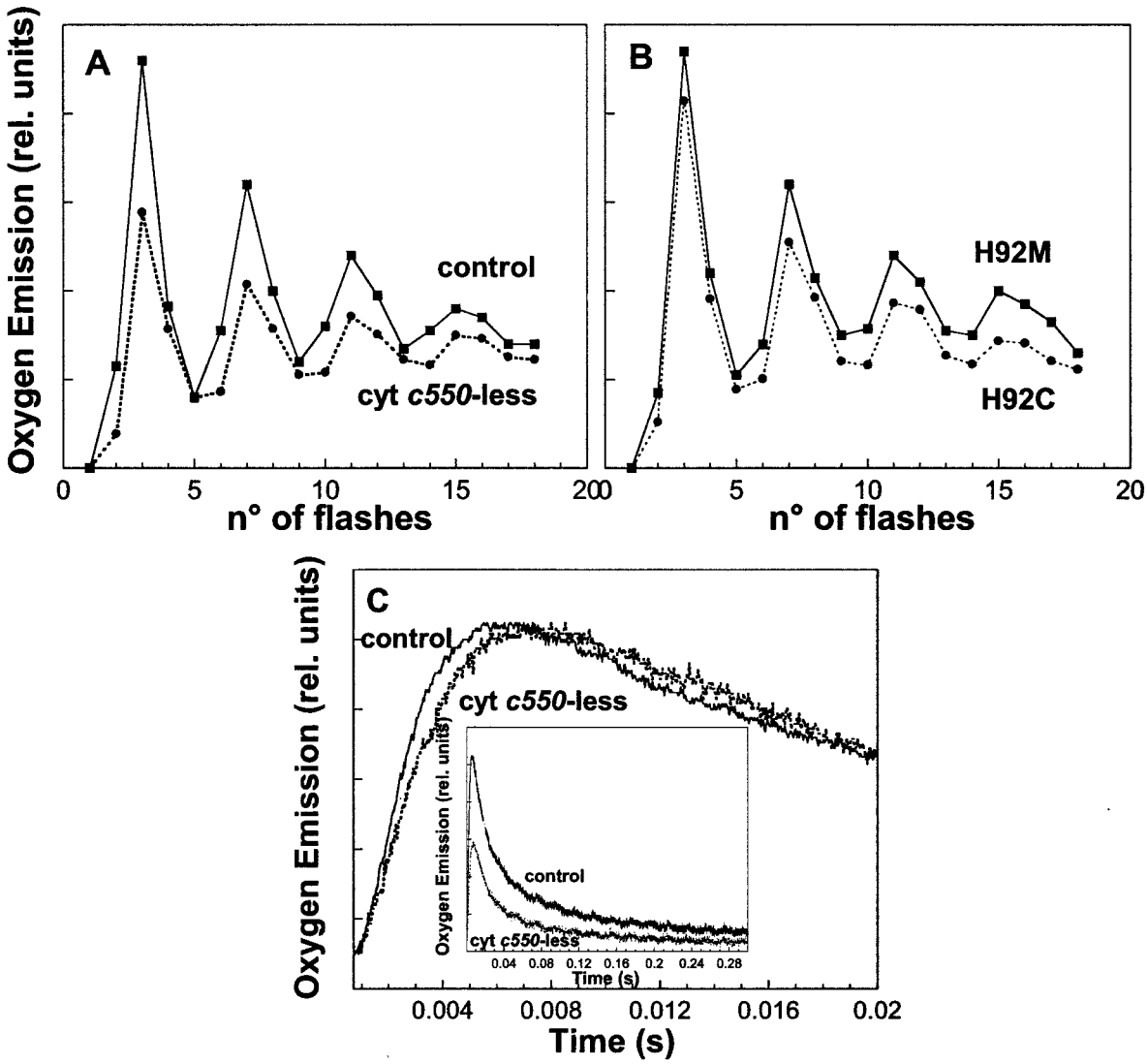

FIG. 5. **Flash-induced oxygen evolution pattern.** Pattern obtained during a sequence of saturating xenon flashes (spaced by 400 ms) using thylakoids of *T. elongatus* control (ΔpsbV2) (*squares*) and cyt *c550*-less (ΔpsbV1) (*circles*) mutants (*A*), thylakoids of *T. elongatus* H92M (*squares*) and H92C (*circles*) mutants (*B*). *C*, oxygen release after the third flash given on thylakoids of *T. elongatus* control (ΔpsbV2) (*solid line*) and cyt c_{550}-less mutant (ΔpsbV1) (*dashed line*). The curves were normalized to the maximum of oxygen released. *Inset*, complete curves without normalization.

oscillates with a period of 4 with a first maximum after two flashes corresponding to the maximum amount of S_2/S_3. $S_3Q_B^-$ luminescence is 1.7 times greater than $S_2Q_B^-$ (37). TL from the control (ΔpsbV2 cells) was identical to that of the wild type (data not shown). The maximum temperature of the B band obtained after one flash (corresponding to $S_2Q_B^-$ recombination) was about 58–60 °C in control and the H92M and H92C mutant cells. The B bands obtained after 2, 3, and 4 flashes were slightly downshifted (56–57 °C) due to the predominance of $S_3Q_B^-$ recombination that occurs at lower temperatures. The intensities of the thermoluminescence B band, and the oscillations were similar in the three strains. In contrast, the intensities of the B bands of the cyt c_{550}-less mutant were significantly lower and the maxima of the bands were markedly shifted to lower temperatures (48–50 °C). The same experiments were done in thylakoids and similar results were obtained (data not shown).

Since the absence of extrinsic proteins renders the PS II more sensitive to high temperatures (38, 39), the stability of the centers was tested by comparing the B bands obtained after incubating the control and cyt c_{550}-less mutant thylakoids for 2 min at 60 °C, for 5 min at 50 °C or for 5 min at 20 °C before flashing. The area and the maximum of the bands were similar (data not shown). Thus, the shift of the B band in the cyt c_{550}-less mutant cannot be explained by an increased PS II sensitivity to high temperatures that could give a weaker emission artificially shifted to a lower temperature and must correspond to a real destabilization of the $S_2Q_B^-$ state.

The kinetics of $S_2Q_B^-$ deactivation were measured by recording thermoluminescence at increasing time intervals after one flash (Fig. 9*C*). Dark-adapted cells (40 °C) were flashed once to form $S_2Q_B^-$. Then, the B band was recorded after various dark periods at 40 °C. Its intensity decreased but its shape and temperature maximum were not significantly altered. The area of the B band obtained just after the flash was taken as 100% of $S_2Q_B^-$. The $S_2Q_B^-$ decrease could be fitted by one exponential in both strains giving a $t_{1/2}$ of about 120 s in control thylakoids and a $t_{1/2}$ of about 80 s in the cyt c_{550}-less mutant thylakoids A better fit was obtained using a double exponential. In this case the dominant, slower phase, had a $t_{1/2}$ of 150 s (cyt c_{550}-less) and 100 s (control) whereas the faster phase had a $t_{1/2}$ of about 25 s and represented 26 and 10% of the total curve in mutant and control thylakoids respectively. This phase may correspond to the reduction of S_2 to S_1 by TyrD (23).

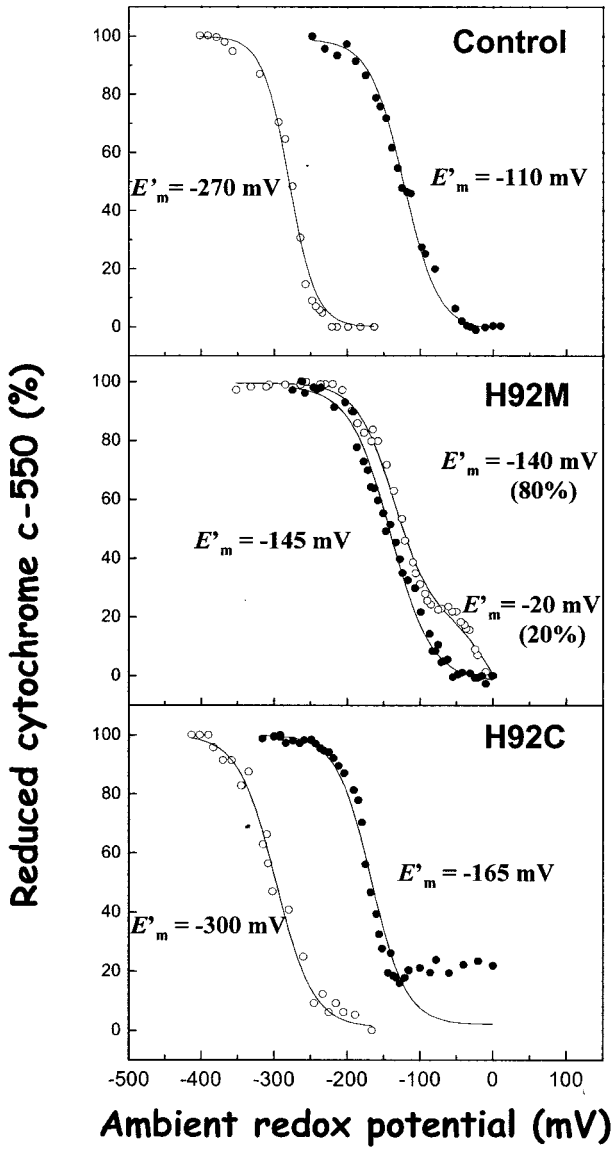

FIG. 6. **Reductive potentiometric titrations.** Plots of the percentages of reduced cyt c_{550} *versus* solution redox potentials obtained from redox titration of unbound (*open circles*) and bound (*closed circles*) cyt c_{550} from control, H92M, and H92C. The *solid curves* represent the best fit of the experimental data to the Nernst equation in accordance with one-electron processes ($n = 1$) for one component. E'_m values shown in the figure were calculated from the Nernst fitting of the reductive potentiometric titration shown in the figure. Each titration was done three times. The E'_m values oscillated about ± 10 mV between the different experiments. Redox titrations were carried out at pH 6.5 as described under "Experimental Procedures."

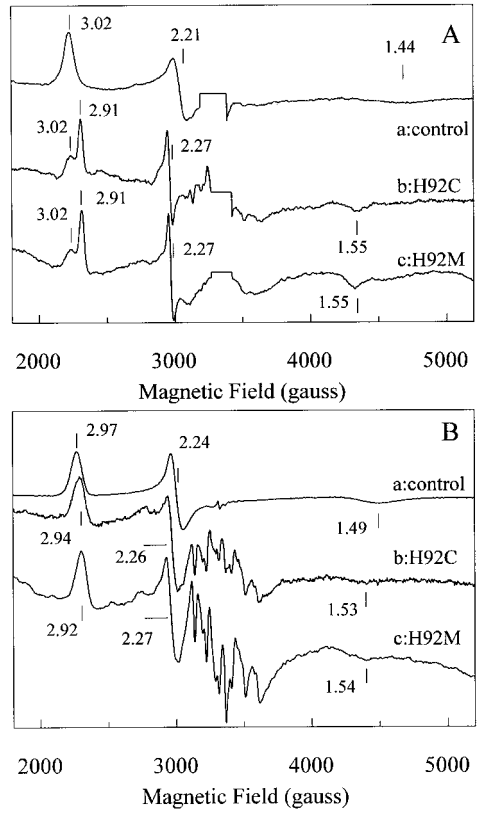

FIG. 7. **EPR spectra of bound (*A*) and isolated (*B*) cyt c_{550}.** CW-EPR spectra of cytochromes bound to PS II (*A*) and isolated (*B*) from *T. elongatus* control, H92C, and H92M strains. *Spectrum a*, control cytochrome; *spectrum b*, H92C cytochrome; *spectrum c*, H92C cytochrome. The amplitudes of the spectra are arbitrary scaled. The center part of the spectra in *panel A* corresponding to the oxidized tyrosine D radical region, was deleted. Instrument settings: temperature, 20 K; modulation amplitude, 20 *G*; microwave power, 2 milliwatts; microwave frequency, 9.4 GHz; modulation frequency, 100 kHz.

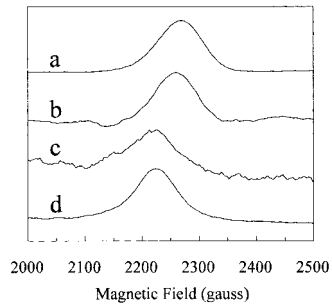

FIG. 8. **EPR spectra of wild-type cyt c_{550} using isolated cytochrome (*spectrum a*), whole cells (*spectrum b*), purified thylakoids (*spectrum c*), and purified PSII (*spectrum d*).** Only the g_z region is shown. Amplitudes of the spectra are arbitrarily scaled. Instrument settings: temperature, 20 K; modulation amplitude, 20 *G*; microwave power, 2 milliwatts; microwave frequency, 9.4 GHz; modulation frequency, 100 kHz.

We also recorded the thermoluminescence bands obtained after flashing the sample in the presence of DCMU (Fig. 9*B*). In this case two bands were detected: one related to $S_2Q_A^-$ recombination (Q band) (34) with a maximum at about 26–28 °C and the other related to $Tyr^{\cdot}Q_A^-$ (C band) (40) with a maximum at 70 °C. No shift to lower or higher temperatures was observed in cells of any mutant. However, in thylakoids a slight (but consistent) upshift (2 °C) of the Q band of the cyt c_{550}-less (ΔpsbV1) mutant was observed (data not shown). In addition, the Q band of the cyt c_{550}-less (ΔpsbV1) mutant was always smaller (in cells and thylakoids) (Fig. 10) and that of the H92C was slightly bigger in cells (Fig. 9) but not in thylakoids (data not shown) compared with that of the control (ΔpsbV2) and the H92M mutant.

Fig. 10 shows the B and Q bands of the isolated PS II complexes. The TL patterns of the control and the H92M PS II isolated centers were similar. Nevertheless, the maxima of the B bands were shifted by about 10 °C to lower temperatures compared with the B bands of cells or thylakoids. This phenomenon was also observed in the wild type (data not shown). This shift could be associated to a change in the lipids due to detergents around the PS II leading to a destabilization of the Q_B binding site and/or the S_2/S_3 states. The fact that a shift to lower temperatures was also detected in the Q band suggests that this effect is caused by an effect on the Mn-cluster rather than on the Q_B binding site. In accordance with its lower

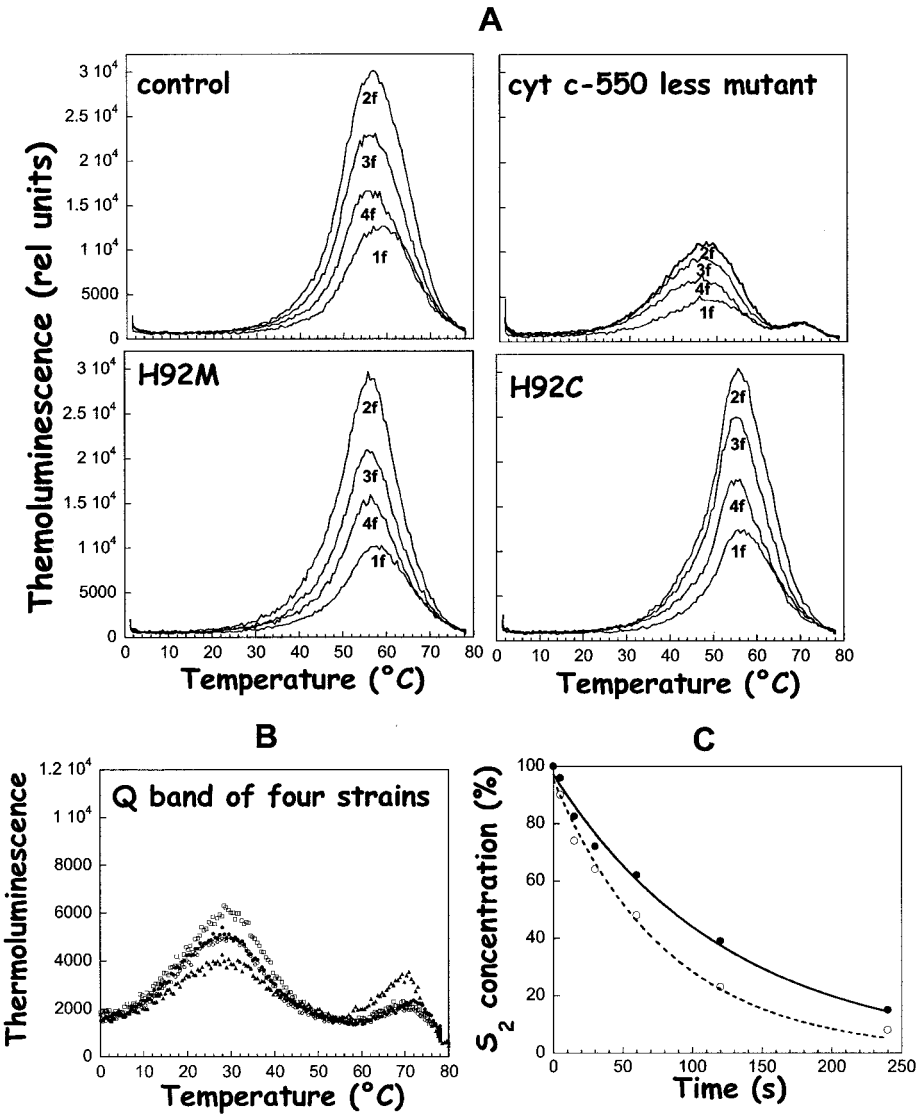

FIG. 9. *A*, thermoluminescence glow curves (B bands) of *T. elongatus* control (ΔpsbV2), cyt *c550*-less mutant (ΔpsbV1), H92M and H92C mutant cells. Cells were maintained on ice in the dark. Before flashing (1–4 flashes) they were dark-adapted for 5 min at 40 °C. The flashes were given at 1 °C. *B*, thermoluminescence glow curves (Q bands) of control (ΔpsbV2) cells (*close circles*), cyt c_{550} less (ΔpsbV1) (*triangles*), H92M (*open circles*), and H92C (*open squares*) mutant cells recorded in the presence of 10 μM DCMU. The flashes were given at −5 °C. *C*, kinetics of $S_2Q_B^-$ deactivation measured by thermoluminescence. 100% S_2 = area of B band obtained just after the flash. The thylakoids were dark-adapted for 5 min at 40 °C then a flash was given (at 40 °C). The TL signals were recorded after various periods of dark at 40 °C.

oxygen evolving activity and its smaller concentration of bound cyt c_{550}, the isolated-PS II complexes from H92C presented smaller B and Q bands (Fig. 10). In addition, a slight downshift (46 °C) of the maximum of the B band was observed. The B bands of the cyt c_{550}-less PS II presented a shift to lower temperatures and were clearly smaller (Fig. 10) compared with control PS II as seen for the B bands of the cyt c_{550}-less thylakoids and cells (Fig. 9).

DISCUSSION

The Cyt c_{550}-less Mutant of T. elongatus—In the present work a cyt c_{550}-less (ΔpsbV1) mutant of *T. elongatus* was constructed. Such a mutant has already been reported but the characterization of the phenotype of this mutant was previously limited to oxygen evolution measurements and to the finding that it was unable to grow in the absence of Cl^- ions (16), a finding confirmed in the present study. In the absence of Ca^{2+}, control cells doubled their concentration while mutant cells did not grow at all suggesting that the absence of the cyt c_{550} has an influence not only on Cl^- binding but also Ca^{2+} binding like in *Synechocystis* PCC 6803 cells.

A further comparison of the cell phenotype of the *T. elongatus* cyt c_{550}-less mutant can be made with literature report of the equivalent mutant in *Synechocystis* PCC 6803 (11). No information is available about PS II activity in thylakoids or isolated PS II complexes from the cyt c_{550}-less *Synechocystis* PCC 6803 mutant. In cells, the decrease in oxygen evolving activity was less marked (35–40% in *T. elongatus versus* 60% in *Synechocystis* PCC 6803), there was no retardation of O_2 release (3 ms in *Synechocystis*), no upshift of the maximum emission temperature of the $S_2Q_A^-$ and S_2 Q_B^- TL bands (10 and 6 °C, respectively, in *Synechocystis* PCC 6803), and no rapid deactivation of the Mn-cluster in the dark (90% in 2 h in *Synechosystis* PCC 6803). These results suggest that the cyt c_{550}-less PS II of the *T. elongatus* is more stable than that of *Synechocystis* PCC 6803 at least in whole cells.

It is very unlikely that the greater stability of the cyt c_{550}-less *T. elongatus*-PS II compared with that in *Synechocystis* PCC 6803 is caused by the presence of the PsbV2 protein. This protein has never been detected in association with PS II and is present in very small quantities (only 1% of soluble cyt c_{550}) (17) in the cells. Furthermore when over-expressed in the cyt c_{550}-less mutant in *Synechocystis*, the PsbV2 protein did not reverse the suppression of growth in the absence of Ca^{2+} or Cl^- ions (16).

Most of the defects seen in PS II activity in the cyt c_{550}-less *Synechocystis* mutant cells were also observed in the *Synechocystis* PCC 6803 mutant lacking the 33 kDa protein (ΔpsbO) (41): notably the upshift of TL bands, the retardation of O_2 release and the rapid deactivation of the Mn-cluster in the dark. Thus, the effects attributed to the lack of cyt c_{550} in

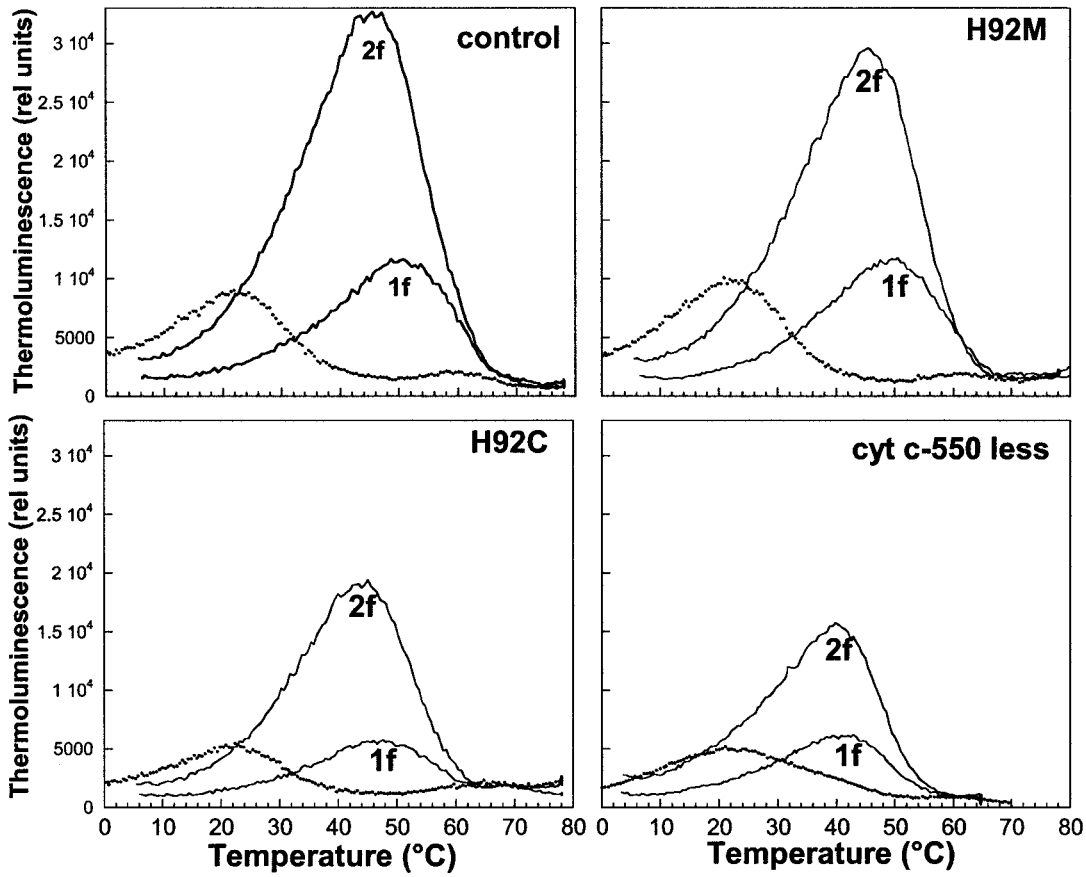

FIG. 10. **Thermoluminescence glow curves of isolated PS II complexes from control, H92M, H92C, and cyt c_{550}-less mutants recorded after 1 and 2 flashes in the absence of DCMU (*solid lines*) or in the presence of 10 μM DCMU (*dotted lines*).**

Synechocystis could at least in part be due to a weaker binding of the 33 kDa (and maybe of the 12 kDa) to the PS II complex even in the cells. It is well known that the binding of the extrinsic proteins is very labile in *Synechocystis* PCC 6803. The isolation of active PS II complexes, even from wild-type cells, is not trivial. While it was possible to isolate active thylakoids from the cyt c_{550}-less *T. elongatus* mutant, changes in PS II properties were induced: notably a slight retardation of O_2 release, a slight upshift of the maximum of the TL Q band and decreased oxygen activity compared with cells. These changes were attributable to the loss or loosening of extrinsic proteins, particularly the 33 kDa.

As already mentioned, when the cyt c_{550}-less mutant from *Synechocystis* PCC 6803 was studied with TL, the $S_2Q_B^-$ and the $S_2Q_A^-$ TL bands were found to be upshifted (11). In contrast, the cyt c_{550}-less *T. elongatus* mutant cells showed no-shift of the $S_2Q_A^-$ TL band and a downshift of the maximum of the $S_2Q_B^-$ recombination TL band. This corresponded to a more rapid decay of $S_2Q_B^-$ in the mutant. Thermoluminescence was reported previously from isolated PS II complexes of *T. vulcanus*, another thermophilic species (4), in which the extrinsic proteins were removed and reconstituted. In PS II with the 33 kDa reconstituted but lacking the cyt c_{550} and the 12 kDa, a shift to lower temperature was seen for the $S_2Q_B^-$ band, in agreement with the present work. Moreover, the upshift of the Q band disappeared after reconstitution with the 33 kDa protein alone, suggesting that the stabilization of the $S_2Q_A^-$ state was related to the lack (or weaker binding) of the 33 kDa protein and not to the lack of the 12 kDa protein as suggested by Shen *et al.* (11). The destabilization of the $S_2Q_B^-$ state could be due to a higher instability of either the S_2 state or Q_B^-, or both. The $S_2Q_A^-$ state appears to be unaffected by the lack of cyt c_{550}. Thus there are two possible explanations that would rationalize the TL results. 1) Q_B^- is destabilized while S_2 and Q_A^- are unaffected, or 2) Q_B^- is unaffected, S_2 is destabilized and Q_A^- is stabilized thus canceling out the effect of S_2 destabilization. Both situations are not without precedence, with donor-side influences on the acceptor side (*e.g.* 42–44) and *vice versa* (45), both are present in the literature.

Another minor modification in the PS II attributable to the absence of the cyt c_{550} was the increased concentration of S_0 in dark-adapted cells (see oxygen per flash results). The cyt c_{550}-less mutant may allow access of reductants to the Mn-cluster, either directly or because of weaker binding of the extrinsic proteins when the cytochrome is absent. Since the slow reduction of the Mn-cluster resulting in formation of S_0 and lower S states will be counteracted by their reoxidation by $TyrD^{\cdot}$ (46), it seems reasonable that higher than normal concentrations of S_0 and lower than normal amounts of $TyrD^{\cdot}$ could occur together under such conditions. The fast phase of $S_2Q_B^-$ decay attributable to electron donation from TyrD is indeed increased in the cyt c_{550}-less mutant.

In conclusion the absence of the cyt c_{550} results in 1) a lowered affinity for Cl^- and most probably Ca^{2+}, 2) a destabilization of the $S_2Q_B^-$ because of donor and/or acceptor side effects, 3) a modification in reactions between the TyrD/$TyrD^{\cdot}$ and the Mn complex, which could be because the Mn-cluster was less well insulated from attack by exogenous reductants, caused by a weaker binding of the other extrinsic proteins.

The Control and the Site-directed Mutated Cyt c_{550}—Shen and Inoue (5) suggested that all the cyt c_{550} present in the cells was attached to the PS II. Here, however, we presented data suggesting that in control whole cells, in addition to the PS II-bound cyt c_{550}, a significant fraction of cyt c_{550} is present in

the soluble form. EPR experiments clearly showed that the g_z-value of the signal corresponding to cyt c_{550} in whole cells was similar to that of isolated cyt c_{550}. The role and cellular localization of this soluble cyt c_{550} is still unknown. However, the fact that the cyt c_{550} isolated from the soluble fraction had lost the transit sequence could suggest that it was present in the lumen and not in the cytoplasm as suggested by its very low redox potential.

In the present work, we substituted the His-92, the sixth axial ligand of the heme iron in cyt c_{550} with a cysteine and a methionine. EPR spectra demonstrated that both mutations resulted in the heme as six-coordinated. However, the *g*-values of the mutated cytochromes were different from those of the wild-type cyt c_{550}, indicating that the environment of the heme was modified. The mutated cytochromes were less stable and more weakly bound to the PS II than the wild-type cyt c_{550}. The change of His to Met in cyt c_{550} led to an increase of the redox potential of about 130 mV. In contrast, in the H92C mutant, the change of His to Cys downshifted the already low E'_m (−270 mV) of the cyt c_{550} about 30 mV. The marked difference in the E'_m of the hemes seen in the isolated mutant cytochromes (H92C = −300 mV, H92M = −140 mV) was much less apparent when they were bound to PS II. (H92C = −165 mV, H92M = −145 mV). In addition, the bound mutated cytochromes presented quite similar EPR spectra (the *g*-values were almost identical), both different from that of the wild-type cyt c_{550}.

The binding of the wild-type cytochrome led to an E'_m increase of about 180–200 mV compared with the isolated cyt c_{550} (14). It was proposed that this large increase in E'_m could be due to a much lower solvent accessibility of the heme when the cyt is bound to the PS II (14). In addition we have proposed that Tyr-82 is responsible for the pH dependence of the redox potential of the soluble cyt c_{550} (14). This pH dependence disappears when cyt c_{550} is bound to PS II. This could be due to either a binding-induced change of the pK_a of the Tyr-82 or a loss of solvent accessibility to this group. Such a low solvent exposure would allow the ionizing group to remain protonated, inducing the more positive E'_m also observed in the soluble cyt c_{550} at low pH values. The recent resolution of the PS II structure at 3.5 Å (8) shows that when bound to PS II the heme pocket is occluded by amino acids chains from the 12 kDa and the CP43 proteins, confirming the lower exposure of the heme to the solvent in the bound cyt c_{550}. Moreover, it is possible that the oxygen of Tyr-82 forms a hydrogen bond with the C-terminal Ile-66 of the 12 kDa protein (8).

The binding of the H92C-mutated cyt c_{550} also resulted in an increase in the E'_m, although this increase was somewhat smaller than in control (135 *versus* 180/200 mV). In contrast, the H92M-mutated cyt c_{550} did not show a binding-induced effect on the E'_m: the redox potential of the bound and unbound cytochrome was around −140 mV. This could be explained by a mutation-induced change in the binding that prevents the usual increase in the E'_m. Alternatively the phenomenon triggered by the binding (*e.g.* a decrease in solvent access or a change in a pK_a of the dominant ionizable group) could already be present in the soluble mutated cytochrome. If the Tyr-82 does play a role, as suggested, it is possible to imagine several scenarios in which the phenomena can be explained, including modifications of its electrostatic environment by exclusion of solvent or other binding effects.

Effect of Point Mutations on PS II Activity—The mutation of the His-92 to Met or Cys did not modify PS II activity. In whole mutant cells and in thylakoids, the oxygen evolving activity, light saturation curves (data not shown), the pattern of oxygen evolved per flash, the thermoluminescence B and Q bands, and the cell growth in the absence of Ca^{2+} or Cl^- were all identical to those in our control strain, the ΔpsbV2 mutant. None of the characteristics of the cyt c_{550}-less mutant were present in the His-92 mutants.

This is also true for the characteristics of the isolated PS II complexes from H92M mutant, which were almost identical to those of the control strain. In the case of the H92C mutant, however, characteristics of the cyt c_{550}-less strain appeared in the isolated PS II complexes, and those were almost certainly caused by the fractional loss of cyt c_{550} implying that the mutated cytochrome was more weakly bound.

Even though the large changes in the redox potential of the mutated unbound cyt c_{550} were damped out to a large extent by the binding of the cytochrome to PSII, smaller but still significant shifts in potential (30–50 mV) were detected in the bound mutated cyt c_{550}. This difference in the redox potential had no influence on PSII activity. This argues against a redox role for this heme in PSII function or in cell growth under the conditions tested. The absence of the cyt c_{550} had more influence on PSII activity but all the effects observed could be explained in terms of a binding role: contributing to the stability and binding of the other extrinsic polypetides, responsible at least in part for maintaining the affinity for the Cl^- and Ca^{2+} ions and possibly acting directly as a barrier to reductive attack on the Mn^{2+}. The role of the heme itself remains enigmatic.

REFERENCES

1. Holton, R. W., and Myers, J. (1963) *Science* **142,** 234–235
2. Kerfeld, C. A., and Krogmann, D. W. (1998) *Annu. Rev. Plant Physiol. Plant Mol. Biol.* **49,** 397–425
3. Shen, J. R., Ikeuchi, M., and Inoue, Y. (1992) *FEBS Lett.* **301,** 145–149
4. Shen, J. R., and Inoue, Y. (1993) *Biochemistry* **32,** 1825–1832
5. Shen, J. R., and Inoue, Y. (1993) *J. Biol. Chem.* **272,** 17821–17826
6. Zouni, A., Witt, H. T., Kern, J., Fromme, P., Krauβ, N., Saenger, W., and Orth, P. (2001) *Nature* **409,** 739–743
7. Kamiya, N., and Shen, J. R. (2003) *Proc. Natl. Acad. Sci. U. S. A.* **100,** 98–103
8. Ferreira, K., Iverson, T., Maghlaoui, K., Barber, J., and Iwata, S. (2004) *Science* **303,** 1831–1838
9. Shen, J. R., Vermaas, W., and Inoue, Y. (1995) *J. Biol. Mol.* **270,** 6901–6907
10. Shen, J. R., Burnap, R. L., and Inoue, Y. (1995) *Biochemistry* **34,** 12661–12668
11. Shen, J. R., Qian, M., Inoue, Y., and Burnap, R. L. (1998) *Biochemistry* **37,** 1551–1558
12. Hoganson, C. W., Lagenfelt, G., and Andréasson, L.-E. (1990) *Biochim. Biophys. Acta* **1016,** 203–206
13. Navarro, J. A., Hervas, M., De la Cerda, B., and De la Rosa, M. A. (1995) *Arch. Biochem. Biophys.* **318,** 46–52
14. Roncel, M., Boussac, A., Zurita, J. L., Bottin, H., Sugiura, M., Kirilovsky, D., and Ortega, J. M. (2003) *J. Biol. Inorg. Chem.* **8,** 206–216
15. Jordan, P., Fromme, H. T., Witt, O. Klukas, W., Saenger, N., and Krauβ, N. (2001) *Nature* **411,** 909–917
16. Katoh, H., Itoh, S., Shen, J. R., and Ikeuchi, M. (2001) *Plant Cell Physiol.* **42,** 599–607
17. Kerfeld, C. A., Sawaya, M. R., Bottin, H., Tran, K. T., Sugiura, M., Cascio, D., Desbois, A., Yeates, T. O., Kirilovsky, D., and Boussac, A. (2003) *Plant Cell Physiol.* **44,** 697–706
18. Sugiura, M., and Inoue, Y. (1999) *Plant Cell Physiol.* **40,** 1219–1231
19. Mühlenhoff, U., and Chauvat, F. (1996) *Mol. Gen. Genet.* **252,** 93–100
20. Golden, J. W., and Wiest, D. R. (1988) *Science* **242,** 1421–1423
21. Cai, Y., and Wolk, C. P. (1990) *J. Bacteriol.* **172,** 3138–3145
22. Miyao, M., Murata, N., Lavorel, J., Maison, B., Boussac, A., and Etienne, A. L. (1987) *Biochim. Biophys. Acta* **890,** 151–159
23. Boussac, A., Rappaport, F., Carrier, P., Verbavatz, J.-M., Gobin, R., Kirilovsky, D., Rutherford, A. W., and Sugiura, M. (2004) *J. Biol. Chem.* **279,** 22809–22819
24. Ducruet, J.-M. (2003) *J. of Exp. Bot.* **54,** 2419–2430
25. Lumry, R., and Rieske, J. S. (1959) *Plant Physiol.* **34,** 301–305
26. Rieske, J. S., Lumry, R., and Spikes, J. D. (1959) *Plant Physiol.* **34,** 293–300
27. Satoh, K., Katoh, S., and Takamiya, A. (1972) *Plant Cell Physiol.* **13,** 885–897
28. Papageorgiou, G. C., Fujimura, Y., and Murata, N. (1991) *Biochim. Biophys. Acta* **1057,** 361–366
29. Mohanty, P., Hayashi, H., Papageorgiou, G. C., and Murata, N. (1993) *Biochim. Biophys. Acta* **1144,** 92–96
30. Joliot, P., Barbieri, G., and Chabaud, R. (1969) *Photochem. Photobiol.* **10,** 309–329
31. Kok, B., Forbush, B., and McGloin, M. (1970) *Photochem. Photobiol.* **11,** 457–475
32. Berthomieu, C., Boussac, A., Mantele, W., Breton, J., and Nabedryk, E. (1992) *Biochemistry* **31,** 11460–11471
33. Blumberg, W. E., and Peisach, J. (1971) in *Probes of Structure and Function of Macromolecules and Membranes* (Chance, B., Yonetani, T., and Mildvan, A. S., eds) Vol. 2, pp. 215–229, Academic Press, New York
34. Rutherford, A. W., Crofts, A. R., and Inoue, Y. (1982) *Biochim. Biophys. Acta*

682, 457–465
35. Vass, I., and Inoue, Y. (1992) in *Topics in Photosynthesis* (Barber, J., ed) Vol. 11, pp. 259–294. Elsevier, Amsterdam, The Netherlands
36. Miranda, T., and Ducruet, J.-M. (1995) *Photosynthesis Res.* **43,** 251–262
37. Rutherford, A. W. Renger, G., Koike, H., and Inoue, Y. (1984) *Biochim. Biophys. Acta.* **767,** 548–556
38. Nishiyama, Y., Hayashi, H., Watanabe, T., and Murata, N. (1994) *Plant Physiol.* **105,** 1313–1319
39. Kimura, A., Eaton-Rye, J. J., Morita, E. H., Nishiyama, Y., and Hayashi, H. (2002) *Plant Cell Physiol.* **43,** 932–938
40. Johnson, G. N., Boussac, A., and Rutherford, A. W. (1994) *Biochim. Biophys. Acta* **1184,** 85–92
41. Burnap, R. L., Shen, J.-R., Jursinic, P. A., Inoue, Y., and Sherman, L. A. (1992) *Biochemistry* **31,** 7404–7410
42. Krieger, A., Weis, E., and Demeter, S. (1993) *Biochim. Biophys. Acta* **1144,** 411–418
43. Johnson, G., Rutherford, A. W., and Krieger, A. (1995) *Biochim. Biophys. Acta* **1229,** 202–207
44. Vass, I., Ono, T.-A., and Inoue, Y. (1987) *FEBS Lett.* **211,** 215–220
45. Kirilovsky, D., Ducruet, J.-M., and Etienne, A.-L. (1991) *Biochim. Biophys. Acta* **1060,** 37–44
46. Styring, S., and Rutherford, A. W. (1987) *Biochemistry* **26,** 2401–2405

Cytochrome c_{550} in the Cyanobacterium *Thermosynechococcus elongatus*: STUDY OF REDOX MUTANTS

Diana Kirilovsky, Mercedes Roncel, Alain Boussac, Adjélé Wilson, Jorge L. Zurita, Jean-Marc Ducruet, Hervé Bottin, Miwa Sugiura, José M. Ortega and A. William Rutherford

J. Biol. Chem. 2004, 279:52869-52880.
doi: 10.1074/jbc.M408206200 originally published online September 22, 2004
